Mapping Wildfire Burn Severity in the Arctic Tundra from Downsampled MODIS Data

Author(s): Crystal A. Kolden and John Rogan
Source: Arctic, Antarctic, and Alpine Research, 45(1):64-76. 2013.
Published By: Institute of Arctic and Alpine Research (INSTAAR), University of Colorado
DOI: http://dx.doi.org/10.1657/1938-4246-45.1.64
URL: http://www.bioone.org/doi/full/10.1657/1938-4246-45.1.64

Arctic, Antarctic, and Alpine Research, Vol. 45, No. 1, 2013, pp. 64–76

Mapping Wildfire Burn Severity in the Arctic Tundra from Downsampled MODIS Data

Crystal A. Kolden and John Rogan†*

*Corresponding author: Department of Geography, University of Idaho, Moscow, Idaho 83844-3021, U.S.A.
ckolden@uidaho.edu
†Graduate School of Geography, Clark University, 950 Main Street, Worcester, Massachusetts 01610, U.S.A.

Abstract

Wildfires are historically infrequent in the arctic tundra, but are projected to increase with climate warming. Fire effects on tundra ecosystems are poorly understood and difficult to quantify in a remote region where a short growing season severely limits ground data collection. Remote sensing has been widely utilized to characterize wildfire regimes, but primarily from the Landsat sensor, which has limited data acquisition in the Arctic. Here, coarse-resolution remotely sensed data are assessed as a means to quantify wildfire burn severity of the 2007 Anaktuvuk River Fire in Alaska, the largest tundra wildfire ever recorded on Alaska's North Slope. Data from Landsat Thematic Mapper (TM) and downsampled Moderate-resolution Imaging Spectroradiometer (MODIS) were processed to spectral indices and correlated to observed metrics of surface, subsurface, and comprehensive burn severity. Spectral indices were strongly correlated to surface severity (maximum $R^2 = 0.88$) and slightly less strongly correlated to substrate severity. Downsampled MODIS data showed a decrease in severity one year post-fire, corroborating rapid vegetation regeneration observed on the burned site. These results indicate that widely-used spectral indices and downsampled coarse-resolution data provide a reasonable supplement to often-limited ground data collection for analysis and long-term monitoring of wildfire effects in arctic ecosystems.

DOI: http://dx.doi.org/10.1657/1938-4246-45.1.64

Introduction

Wildfires are historically rare in the arctic tundra (Wein, 1976), but new evidence of more frequent fires during Holocene warm periods suggests wildfire activity may increase significantly due to relatively rapid climate change (Higuera et al., 2008). Observed warming trends over the past 50 years have impacted the high latitudes (>60°) more rapidly than elsewhere on earth (Serreze et al., 2000; Hinzman et al., 2005; IPCC, 2007), fostering concerns over the fate of ecosystems and endangered species in those regions (e.g., O'Neill et al., 2008; Durner et al., 2009), and the one-third of global terrestrial carbon stocks that are sequestered in boreal biomes (Apps et al., 1993; Kasischke, 2000).

Across the North American Arctic, surface air temperature increased 1.09 °C per decade (±0.22 °C) from 1981 to 2000 (Cosimo, 2006). In Alaska, this warming trend is attributed to the advance of spring snowmelt (by 9.1 days per decade for the Arctic coastal plain, referred to as the 'North Slope') (Chapin et al., 2005), an observed 6% increase in tall shrub cover across the North Slope over the last 50 years, which lowers surface albedo (Chapin et al., 2005; Sturm et al., 2005), and an observed treeline advance into the Alaskan tundra (Lloyd and Fastie, 2003). The feedbacks produced by these observed changes, including increasing wildfire activity, thawing permafrost, and further shrub expansion, are expected to amplify general warming trends and changes in the tundra environment (Chapin et al., 2005; Hinzman et al., 2005).

Only 20 wildfires had been recorded prior to 2007 on Alaska's North Slope, and research addressing wildfire effects on tundra has primarily been limited to Alaska's western coastline and on the Seward Peninsula. In 2007, four wildfires occurred on the North Slope, including the record 103,000 ha Anaktuvuk River Fire. This event provided dramatic evidence supporting the hypothesis of increased wildfire activity resulting from climate change (Jones et al., 2009). Alaska land managers, concerned with fire effects on wildlife conservation efforts, carbon sequestration, and natural resource management, concurrently expressed a need for reproducible methods to monitor wildfire impacts in remote regions (Allen and Sorbel, 2008; Murphy et al., 2008) where growing seasons span less than 4 months and ground data collection in roadless areas is challenging and expensive (Bogdanov et al., 2005).

Remotely sensed data have been widely utilized to characterize wildfire regimes in ecotypes with characteristics similar to tussock tundra. For example, fire histories have been mapped using remotely sensed data in grasslands dominated by tussock-building species (Curry, 1996; Allan, 1993; Russell-Smith and Yates, 2007), but fire effects in tussock tundra have not been quantified from spaceborne imagery (*but see* Allen and Sorbel, 2008). In Alaska, efforts have focused on utilizing remotely sensed data to map various fire effects metrics in black spruce (*Picea mariana*) forests (Epting et al., 2005; Hudak et al., 2007; Hoy et al. 2008; Kasischke et al., 2008, Murphy et al.; 2008), but have largely ignored tundra wildfires, since most (94%) of area burned in Alaska during the historic period was located in the boreal forest interior region (AFS, 2009). Much recent wildfire research has been devoted to burn severity mapping and, specifically, developing methods and indices for delineating burn severity from remotely sensed data (White et al., 1996; Rogan and Yool, 2001; Rogan and Franklin, 2001; Miller and Thode, 2007), but these methods have not yet been tested for the arctic tundra. As there is no agreed-upon definition of burn severity at present time (Keeley, 2009), we define it for this study as the proportional fire-induced ecological change aggregated across and captured by the multispectral reflectance of a pixel.

1523-0430/6 $7.00

In Alaska, it is challenging to collect ground ecological observations, resulting in relatively small sample sizes and difficulty accurately classifying remotely sensed data. Classification accuracy is further reduced by errors in geometric registration (Verbyla and Boles, 2000), a short (2–4 months) growing season (Stow et al., 2004), topographic shadowing due to steep terrain and low sun angles (Verbyla et al., 2008), and significant Landsat data gaps prior to the construction of a receiving station in 2005 (French et al., 2008). An additional challenge specific to burn severity mapping is that the advancement of the growing season can vary by several weeks (Markon, 2001; Stow et al., 2004), and vegetation regeneration can occur within days after a fire and before post-fire imagery can be acquired (French et al., 2008; Allen and Sorbel, 2008). More complex burn severity mapping approaches (i.e. Rogan and Franklin, 2001; De Santis and Chuvieco, 2009) have produced more accurate burn severity maps than those derived from linear indices alone. However, linear spectral indices continue to be the most desirable to land managers due to their reproducibility and low processing requirements (Zhu et al., 2006; Murphy et al., 2008). As such, the differenced Normalized Burn Ratio (dNBR) was selected for development of a national burn severity atlas in the U.S.A. (Eidenshink et al., 2007).

To date, the dNBR is the only spectral reflectance index that has been assessed for its ability to reflect ground observations of wildfire burn severity in the tundra and was only tested for representation of a composite measure of burn severity (Allen and Sorbel, 2008) with moderately good correlation ($R^2_{adj} = 0.81$). The dNBR and other burn severity mapping indices produce higher correlations to ground measurements of burn severity data when indices are derived from relatively high-resolution spectral data, (e.g., Landsat Thematic Mapper [TM]) rather than lower resolution data [i.e., Moderate resolution Imaging Spectroradiometer (MODIS)] (Walz et al., 2007; Boelman et al., 2011). However, the short growing season (Stow et al., 2004) and 93–100% cloud cover during the growing season months (Intrieri et al., 2002) limit Landsat data acquisition in the Arctic.

The primary objective of this study was to address the collective challenges of mapping burn severity on the arctic tundra by testing published spectral indices and assessing the utility of a high-temporal, moderate-spatial resolution sensor in conjunction with a recently developed downsampling method in order to characterize the historic 2007 Anaktuvuk River wildfire that occurred on the North Slope of Alaska at high resolution (i.e., 30 m). MODIS is widely used to monitor fire occurrence and fire effects due to its daily temporal resolution (Kaufman et al., 2003) and recent efforts have produced data fusion techniques that downsample 500 m MODIS data to the spatial resolution of higher resolution sensors (Gao et al., 2006). The goals of this study were to (1) correlate established spectral indices to ground observations of tundra burn severity; (2) demonstrate downsampled MODIS as an alternative to Landsat for mapping and monitoring wildfire characteristics in a data-poor region; and (3) characterize the burn severity of the historic Anaktuvuk River Fire in the context of other tundra wildfires.

Wildfire in the Arctic Tundra

Wildfires are a primary ecological disturbance in boreal ecosystems (Wein and MacLean, 1983; Kasischke and Stocks, 2000; Chapin et al., 2006), but wildfire impacts on wildlife habitat, vegetative trajectories, and carbon cycles are poorly understood in the arctic tundra due to their historical infrequency and a lack of empirical research studies (Wein, 1976; Jones et al., 2009). The Alaska Fire Service (2009) recorded only 24 wildfires on the North Slope region from 1950 to 2008 (20 from 1950–2006, plus 4 in 2007) with the fires burning a mean area of 6240 ha, but a median area of only 115 ha (i.e., an anomalous 103,000 ha wildfire in 2007 skewed the mean value). Historic North Slope fire frequency is unknown since only large fires (>400 ha) were recorded prior to 1989 (AFS, 2009), but mean fire frequency was 144 years (± 90) during the early Holocene between 10,000 and 14,000 years BP (Higuera et al., 2008), and at two sites in the Anaktuvuk River Fire area, there is no evidence of wildfires to 5000 years BP (Hu et al., 2010).

Previous research on tundra wildfire impacts focused solely on a spate of 1977 and 2002 wildfires on the western Alaska Coastal Plain and in the Noatak River watershed (Racine et al., 1987, 2004; Liljedahl, et al., 2007). The western coastal region is climatically distinct from the North Slope of Alaska in that it receives two to three times as much annual precipitation, is an average of 5–10 °C warmer than the North Slope, and is subject to a different synoptic pattern more conducive to lightning during fire season (Shulski and Wendler, 2007; Murphy and Witten, 2008; WRCC, 2009). Despite similar vegetation types, the North Slope has a history of significantly fewer and less frequent fires. However, projected warming trends for the North Slope (IPCC, 2007) suggest that fire occurrence and extent on the North Slope may increase, and studies are needed to assess the differences in fire regimes and fire impacts between the two regions, which span nearly 1000 km from the western edge of the Seward Peninsula across the North Slope.

Data and Methods

STUDY AREA

In 2007, the 103,000 ha Anaktuvuk River Fire burned across the arctic tundra on Alaska's North Slope. The fire burned in Brooks Range foothills, a region dominated by cold winters (-25 °C mean high in January), cool summers (20 °C mean high in July), and 14 cm average annual precipitation. Discovered on 16 July, the lightning-ignited fire burned for an estimated 3 months. The peak burning period occurred during a 3-week, anomalous, late-season drought in early September, when annual herbaceous vegetation had already senesced and temperatures were 5–10 °C above normal (Jones et al., 2009).

The Itkillik River and the Anaktuvuk and Nanushuk Rivers confined the fire to the east and west, respectively (Fig. 1). More than 80% of the fire burned vegetation identified by the National Land Cover Database (NLCD) as dwarf scrub, more commonly referred to as 'tussock tundra' due to the dominance of the sedges that form tussocks and low shrubs (Viereck et al., 1992). The dominant vegetation types include willow (*Salix* spp.), Labrador tea (*Ledum palustre*), blueberry (*Vaccinium* spp.), and birch (*Betula nana*) that grow as shrubs, and cottongrass (*Eriophorum* spp.) and other sedges (*Carex* spp.) that form thick, dense tussocks. Rhizomatous tussock-building sedges cover the tundra uplands and can regenerate within weeks after burning (Allen and Sorbel, 2008), while

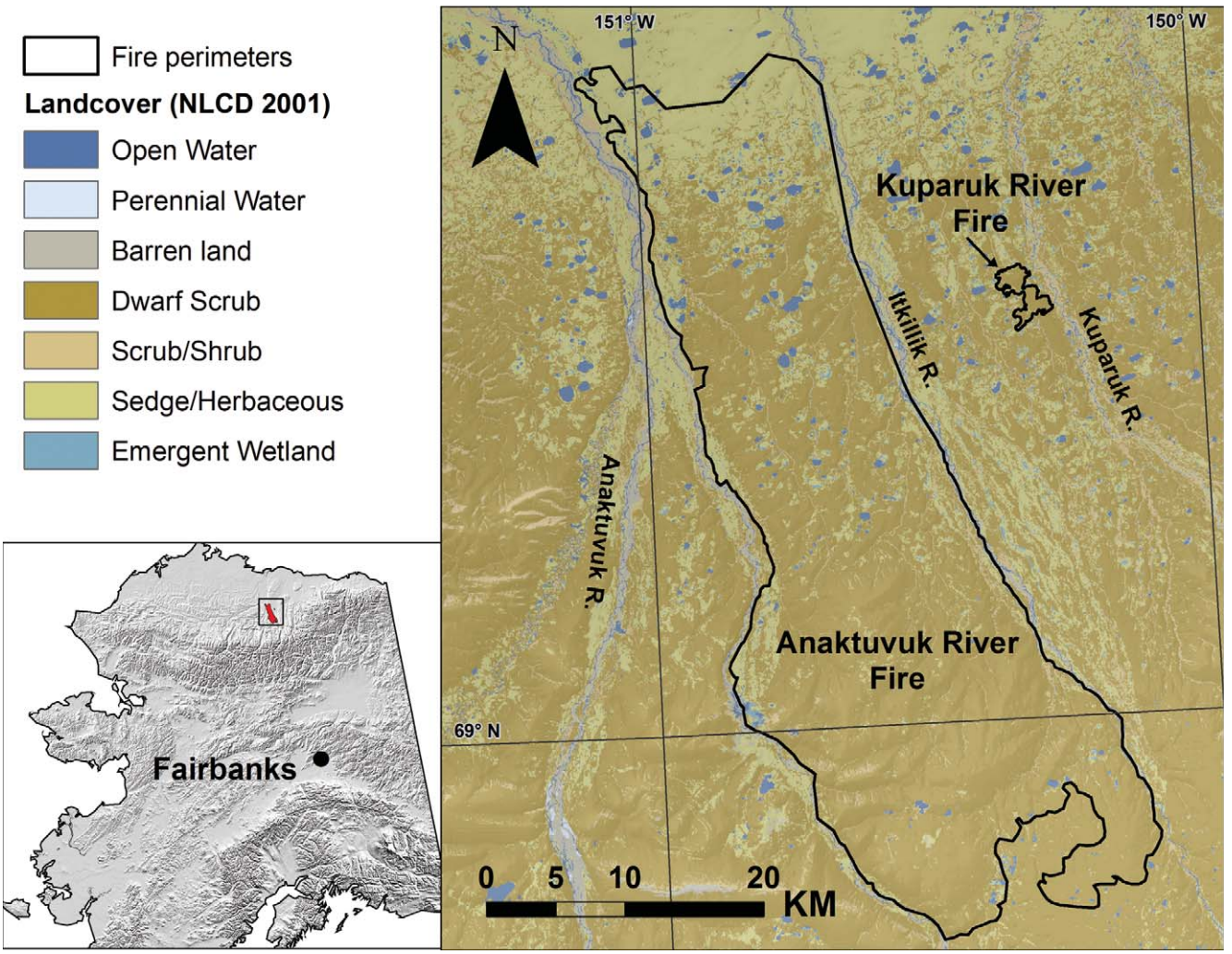

FIGURE 1. Location and dominant land cover (Homer et al., 2007) of the Anaktuvuk River and Kuparuk River wildfires of 2007.

shrubs regenerate to pre-fire levels within 10–25 years (Racine et al., 2004). Lichen species comprising critical winter forage for the Central Arctic Caribou Herd can take up to 120 years to recover from wildfire, depending upon climate variability (Jandt and Myers, 2000). Depth of organic horizon soil consumption by wildfire also determines post-fire permafrost dynamics, which Racine et al. (2004) linked to post-fire vegetation regeneration.

THE ANAKTUVUK RIVER FIRE SCENE MODEL

Strahler et al. (1986) described the utility of developing a scene model for analysis of remotely sensed data: a precise description of what the sensor ''sees'' at the time of image acquisition. Efforts to map burn severity in the U.S.A. have focused on two temporal periods (Zhu et al., 2006). The 'Initial Assessment' is the period following fire containment but prior to any vegetation regeneration. Ideally, post-fire image acquisition for this period occurs immediately following containment, but in Alaska fire containment usually occurs too late in the year for imagery acquisition due to snowfall and low sun angles. In this case, imagery for the Initial Assessment is acquired after snowmelt but prior to green-up the year following the fire. The 'Extended Assessment' occurs after green-up, preferably at peak phenology, one year post-fire. Using both of these assessments in combination allows land managers to assess both primary fire effects (i.e., vegetation and fuel consumption) and secondary fire effects (i.e., resprouting, invasion, erosion).

Here, we describe the scene for three temporal periods: the pre-fire period, the Initial Assessment post-fire (pre-green up), and the Extended Assessment post-fire (post-green up). The pre-fire scene described the landscape at peak phenology during the middle of the growing season. As the Anaktuvuk River Fire was not contained until the first snowfall in late September 2007, the Initial Assessment period for this fire occurred in June of 2008, after snowmelt but prior to green-up. The Extended Assessment scene model is for the peak of phenology in early July 2008 and coincides with the collection of ground burn severity observations.

The pre-fire scene consisted of low-lying herbaceous material (including grass tussocks) on less productive sites or continuous dwarf shrub canopy normally <1 m in height on more productive sites (Fig. 2, part a). Bare soil is not a component of the pre-fire scene in this ecotype, as an organic horizon of decomposing biomass covers the mineral soil. The Initial Assessment (June 2008) post-fire scene (Fig. 2, part b) corresponds with the first available post-snowmelt 2008 Landsat image, and was acquired one year

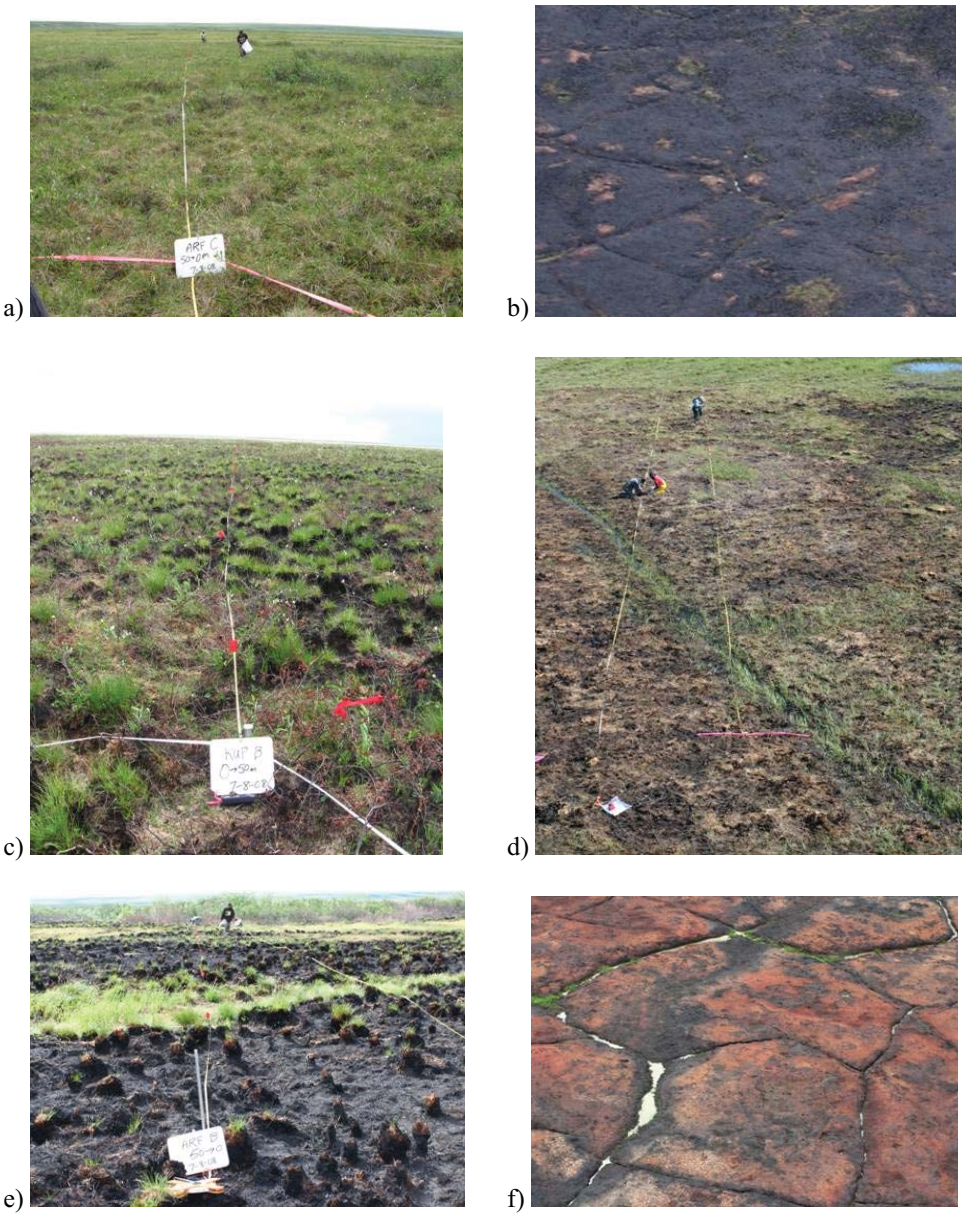

FIGURE 2. Arctic tundra burn severity scene model components for the fire include: (a) unburned pre-fire, (b) post-fire but pre-green-up, (c) low severity plot with unburned inclusions, (d) moderate severity with elements of char and non-photosynthetic vegetation (NPV), (e) post green-up, with tussock regeneration, and (f) high severity with example of oxidized soils. Photos courtesy of R. Jandt, Alaska Fire Service.

after the fire but before the 2008 green-up due to a colder-than-normal June (WRCC, 2009). Observations prior to and during field data acquisition were of standing water, burned and saturated char and black soil surfaces, and patches (sub-meter to several meters in area) of unburned or only partially consumed non-photosynthetic vegetation (NPV), consisting primarily of grasses from prior growing seasons. The organic horizon was consumed in a spatially variable pattern up to a meter in depth (Jandt, 2008).

Some tussock regeneration had occurred by the Extended Assessment (July 2008), adding photosynthetic vegetation (PV) to the scene. On lower severity sites, the fire consumed <20% of the tussock basal area, and unburned mosses interspersed scorched herbaceous cover (Fig. 2, part c). On moderate severity sites, most of the surface was charred, minimal litter was present, the organic duff layer had been irregularly consumed in patches, and the fire had burned 20–60% of the tussock basal area, leaving irregular remnants (Fig. 2, part d). On higher severity sites, >60% of the tussock basal area was consumed, leaving columnar ''stumps'' and deep duff consumption. These sites comprised mostly of char, but some tussock sedges regenerated by early July (Fig. 2, part e). In some sites, all organic material had been consumed to mineral soil, which oxidized to a reddish color (Fig. 2, part f).

DATA

Field Data

The Bureau of Land Management (BLM) established 17 Composite Burn Index (CBI) (Key and Benson, 2006) plots during the first week of July 2008 in the area burned by the Anaktuvuk River Fire and 2 in the smaller (740 ha), nearby Kuparuk River Fire

burned area. The latter 2 plots were established to ensure that lower severity plots were included in the observations (Jandt, 2008). Each plot was located using a preliminary assessment of homogeneity (Jandt, 2008) to be representative of a larger (minimum 90 × 90 m) area of homogeneous burn severity, and were located >500 m apart for all but 2 plots. The plots were sampled using a modified CBI protocol for Alaskan tundra (Allen and Sorbel, 2008). Three measurements of severity were correlated to spectral indices: surface severity (SURF), substrate severity (SUB), and composite severity (CBI). While the number of ground plots is too small to be considered an adequate representative sample that will produce significant correlations, it is representative of the considerable challenge faced by researchers attempting to collect surface data in Alaska.

Sensor Data

Since the ecological scene model is quite different for the Initial (June 2008) versus Extended (July 2008) assessments for the Anaktuvuk River Fire, it was imperative that remotely sensed data be acquired to best represent each time period of the scene model. Ideally, the Initial Assessment would have utilized June 2007 pre-fire and June 2008 post-fire imagery, while the Extended Assessment would have utilized July 2007 pre-fire and July 2008 post-fire imagery. However, few relatively cloud-free Landsat scenes were available during the growing season for the region for either the pre- or the post-fire periods. A pre-fire image was acquired for World Reference System 2 (WRS-2) path 74, row 11, on 14 July 2001 by the Landsat-7 Enhanced Thematic Mapper-Plus (ETM+) sensor. A June post-fire image (corresponding to Initial Assessment) was acquired for WRS-2 path 75, row 11, on 14 June 2008 by the Landsat-5 Thematic Mapper (TM) sensor. Data were pre-processed to 30 m resolution by U.S. Geological Survey (USGS) EROS data center to Level 1T, including geometric, terrain, and radiometric correction to top-of-the-atmosphere reflectance (USGS, 2011). Each image was corrected for atmospheric scattering using dark object subtraction (Chavez, 1996), and converted to at-surface reflectance (Chander and Markham, 2003).

MODIS data were acquired both contemporaneous to the two Landsat acquisition dates, and also corresponding to the ''missing'' optimal time periods that were not covered by available Landsat imagery (Table 1). MOD09A1 8-day 500 m at-surface reflectance data (Vermote and Kotchenova, 2008) were acquired for July 2001 and June 2008 as inputs to the downsampling algorithm, for June 2007 to represent the optimal pre-fire date for the Initial Assessment, and for July 2007 and 2008 to represent the optimal pre- and post-fire dates for the Extended Assessment, following best practices for image selection (i.e., cloud-free, anniversary-date, sun angle, and peak phenology) as described by Key (2006). MODIS data were downsampled to 30 m Landsat spatial resolution using the Spatial and Temporal Adaptive Reflectance Fusion Model (STARFM) (Gao et al., 2006). STARFM is used to develop a quantitative link between a 30 m Landsat image and a concurrent 500 m MODIS image, and downsample the MODIS scene down to the finer 30 m resolution for a date when no Landsat scene exists using that relationship. Quirino et al. (2008) demonstrated the applicability of STARFM for deriving finer resolution Normalized Differenced Vegetation Index (NDVI) products, but the method has not yet been assessed for burn severity mapping. Due to the significant change between the pre-fire and the post-fire scene, pre-fire MODIS images (June and July 2007) were downsampled using the July 2001 pre-fire Landsat image, while the post-fire MODIS image was downsampled using the June 2008 post-fire Landsat image (Table 1).

TABLE 1

Image dates and pairings created to test the utility of downsampled MODIS data modeled from the STARFM algorithm (Gao et al., 2006).

Pair ID	Pre-fire Data	Post-fire Data
Landsat-only	Landsat ETM+ 14 July 2001 Path/Row 74/11 (Concurrent MODIS for STARFM input: Tile h12v02, 2001-193*)	Landsat TM 14 June 2008 Path/Row 75/11 (Concurrent MODIS for STARFM input: Tile h12v02, 2008-169*)
Inital Assessment	STARFM-MODIS 2007-161* Tile h12v02	Landsat TM 14 June 2008 Path/Row 75/11
Extended Assessment	STARFM-MODIS 2007-185* Tile h12v02	STARFM-MODIS 2008-185* Tile h12v02

*Julian day 161 = 10 June; 169 = 18 June; 185 = 4 July; 193 = 12 July.

For both the Initial Assessment and the Extended Assessment, 10 bi-temporal, differenced spectral metrics of burn severity were produced. Some previous Alaska burn severity studies have found single-date, post-fire only indices (e.g., NBR) to produce strong correlations to ground observations (Epting et al., 2005; Hudak et al., 2006; Hoy et al., 2008; Boelman et al., 2011). These studies, however, neglected the primary reason for using a differenced index: the misclassification of non-flammable features. Water surfaces (of high abundance on the North Slope), bare soil, and rock outcroppings often appear as high burn severity in a post-fire image, but fall into the unchanged/unburned category in differenced images (Key, 2006). Since validation plots are never placed in water features, correlations between plots and indices fail to capture this.

Nine bi-temporal, differenced indices (denoted by 'd') and one bi-temporal, relative difference index (denoted by 'Rd') were calculated for three image combinations (Table 2) using the best practices for production and normalization of bi-temporal change indices outlined in Key (2006) and Zhu et al. (2006). For each index, pre-fire and post-fire images were produced, and the post-fire subtracted from the pre-fire to calculate the difference. Indices included two SWIR/NIR band ratios involving Landsat TM bands 7, 5, and 4 (d7/5 and d7/4) and the Normalized Burn Ratio (dNBR and RdNBR). The differences in individual scene components were also assessed utilizing the Kauth-Thomas tasseled cap transformation using coefficients from Mather (1989) and Huang et al. (2001) to transform TM and ETM+ data, respectively, into brightness (dKTB), greenness (dKTG), and wetness (dKTW).

Linear Spectral Mixture Analysis (SMA) was utilized to calculate the fraction and subsequent change of each pixel covered by

TABLE 2

Spectral indices assessed for correlation with burn severity metrics. Equations for the production of the single date transforms or indices are listed first, then the equation given below for the bi-temporal spectral index.

Single-Date Product	*Identifier*	*How Produced (Landsat TM/ETM+ bands where applicable)*
Band 7/Band 4 Ratio	**7/4 Ratio**	(B7) ÷ (B4)
Band 7/Band 5 Ratio	**7/5 Ratio**	(B7) ÷ (B5)
Char fraction of SMA	**CHAR**	Fraction of pixel area from SMA
Green vegetation fraction of SMA	**GV**	Fraction of pixel area from SMA
Non-photosynthetic fraction of SMA	**NPV**	Fraction of pixel area from SMA
Kauth-Thomas Brightness Tranform	**KTB**	TM coefficients from Mather (1989); ETM+ coefficients from Huang et al. (2002)
Kauth-Thomas Greenness Transform	**KTG**	
Kauth-Thomas Wetness Tranform	**KTW**	
Normalized Burn Ratio	**NBR**	(B4 − B7) ÷ (B4 + B7) * 1,000
Bi-temporal Spectral Indices	***Metric ID***	***Form***
Change in 7/4 Ratio	**d7/4**	(Pre-Fire) − (Post-fire)
Change in 7/5 Ratio	**d7/5**	
Change in CHAR fraction	**dCHAR**	
Change in GV fraction	**dGV**	
Change in NPV fraction	**dNPV**	
Change in KTB	**dKTB**	
Change in KTG	**dKTG**	
Change in KTW	**dKTW**	
Change in NBR	**dNBR**	
Relative Change in NBR	**RdNBR**	$\frac{\text{(Pre-Fire NBR) − (Post-Fire NBR)}}{\text{SQRT (ABS(Pre-fire NBR ÷ 1,000))}}$

the scene components char (dCHAR), photosynthetic vegetation (dPV), and non-photosynthetic vegetation (dNPV). In both forested and non-forested ecotypes where components of a burn severity scene occur at sub-pixel resolution, SMA has been shown as a more robust method for enhancing change than traditional approaches such as pixel-based vegetation indices or tasseled cap transforms (Rogan and Franklin, 2001; Rogan et al., 2002; Hudak et al., 2007). The SMA technique utilizes spectral angle mapping to calculate the fraction of each ''pure'' end member present in a given pixel via disaggregating distinct spectral reflectance signatures (Roberts et al., 1998). This study follows Hudak et al. (2007) in using three end members to represent the primary components of the scene: PV, NPV, and CHAR.

To derive reference end-member spectra, indices were used to identify large groups of potential candidates that were then thinned using purification techniques and compared to published reference spectra. The KTG transform and an Enhanced Vegetation Index image were used to identify highly photosynthetic pixels, and the B7/B5 and a B5/B4 ratio image were utilized to define areas of high NPV. An image summing reflectance across bands and a dNBR image were used to delineate CHAR as the pixels where the lowest sum reflectance but the highest dNBR were found. A principal components analysis was performed to further refine homogeneous target areas for training polygons. A pixel purification technique using a Mahalanobis distance typicality threshold (Clark Labs, 2010) was used to remove pixels and reduce training polygon variance, and a mean reflectance signature calculated for each polygon. Library spectra were used to further thin candidates and derive a mean-reflectance spectral signature for the three end members, and each single-date pre- and post-fire image was spectrally unmixed into fraction images of PV, NPV, and CHAR.

The 10 spectral metrics were derived from three sets of image pairs in order to compare Landsat to downsampled MODIS (both 30 m resolution) (Table 1). The Landsat-only pair utilized the July 2001 Landsat image for pre-fire and the June 2008 Landsat image for post-fire. The Initial Assessment pair utilized the downsampled June 2007 MODIS image for pre-fire and the June 2008 Landsat image for post-fire. The Extended Assessment pair utilized the downsampled July 2007 MODIS image for pre-fire and the downsampled July 2008 MODIS image for post-fire.

METHODS

Since the small number of CBI plots (19) is less robust and resistant to outliers as compared to a larger data set, two types of correlation were utilized to assess links between the plot data and the spectral data. Both Pearson product moment coefficients of correlation (ordinary correlation) and the Spearman rank correlation coefficients (rank correlation) were calculated between the 3 CBI metrics (SURF, SUB and CBI) and the 10 spectral metrics (Table 2). Spearman rank correlation is more robust and resistant to outliers and is often used for assessment of small data sets (Wilks, 1995).

To assess the utility of MODIS downsampling in delineating Initial versus Extended Assessments, correlations of CBI metrics were made to the 10 spectral metrics derived for each of the three image pairs: the Landsat-only pair, the Initial Assessment pair, and the Extended Assessment pair. Additionally, the dNBR image for each of the three image pairs (Landsat-only, Initial, and Extended Assessment) was classified into 5 severity classes: Unburned (UNB), Low (LOW), Moderate (MOD), High (HIGH), and Extreme (EXT) severity using a statistical approach that identified

class thresholds as standard deviations from a median value for the entire Landsat scene (as opposed to the arbitrary thresholds identified by MTBS). Since most of the Landsat scene was unburned, the median dNBR value for the Landsat-only pair was normalized to 0 (s.d. = 244). The UNB class included pixels with a dNBR of −244 to +244 (1 s.d.), LOW from 245 to 488 (2 s.d.), MOD from 489 to 732 (3 s.d.), HIGH from 733 to 976 (4 s.d.), and EXT for all pixels greater than 976. These classes were compared to the CBI data and found to match the generalized severity observations made on the CBI plots, and the resulting severity map confirmed as representative of the fire more broadly by the BLM fire ecology expert who had made several flights over the region in the months following the fire (R. Jandt, personal communication). Once each of the 3 image pairs was classified, a confusion matrix was produced to compare the Initial and Extended Assessment pairs to the Landsat-only pair. This confusion matrix describes the change in burn severity associated with one year of regeneration post-fire.

Results

CORRELATIONS BETWEEN CBI METRICS AND SPECTRAL INDICES

Several spectral metrics were significantly correlated to the three metrics of burn severity (Table 3). The Surface (SURF) metric of severity produced the strongest correlations to spectral indices, with a peak R^2 value of 0.880 between dNBR produced from the Landsat-Landsat (L-L) image pair and SURF ($p < 0.0001$). The Substrate (SUB) metric was less strongly correlated, and the CBI (summary metric) correlations fell in between SURF and SUB. The dKTG spectral index produced the strongest correlations to the SUB metric for both the L-L image pairs and the Initial Assessment (IA) image pair ($R^2 = 0.812$, $p < 0.0001$), but RdNBR

TABLE 3

Correlations (R^2) between the 10 spectral metrics and the 3 metrics of burn severity: Surface (SURF), Substrate (SUB), and Composite Burn Index (CBI). Correlations with *p*-values less than 0.001 are considered highly significant.

	SUB		SURF		CBI	
	R^2	*p*	R^2	*p*	R^2	*p*
Landsat-only pair						
d7/4 Ratio	0.553	*0.0003*	0.663	*0.0000*	0.625	*0.0001*
d7/5 Ratio	0.565	*0.0002*	0.678	*0.0000*	0.630	*0.0000*
dKTB	0.514	*0.0006*	0.677	*0.0000*	0.600	*0.0001*
dKTG	0.812	*0.0000*	0.873	*0.0000*	0.863	*0.0000*
dKTW	0.021	*0.5521*	0.083	*0.2307*	0.044	*0.3899*
dCHAR	0.454	*0.0016*	0.541	*0.0003*	0.504	*0.0007*
dPV	0.031	*0.4697*	0.056	*0.3300*	0.042	*0.3988*
dNPV	0.536	*0.0004*	0.610	*0.0001*	0.583	*0.0001*
dNBR	0.772	*0.0000*	0.880	*0.0000*	0.847	*0.0000*
RdNBR	0.775	*0.0000*	0.864	*0.0000*	0.839	*0.0000*
Initial Assessment						
d7/4 Ratio	0.547	*0.0003*	0.658	*0.0000*	0.619	*0.0001*
d7/5 Ratio	0.502	*0.0007*	0.626	*0.0001*	0.570	*0.0002*
dKTB	0.514	*0.0006*	0.677	*0.0000*	0.600	*0.0001*
dKTG	0.812	*0.0000*	0.872	*0.0000*	0.863	*0.0000*
dKTW	0.021	*0.5522*	0.083	*0.2307*	0.044	*0.3900*
dCHAR	0.059	*0.3175*	0.164	*0.0853*	0.101	*0.1849*
dPV	0.055	*0.3322*	0.005	*0.7823*	0.026	*0.5059*
dNPV	0.306	*0.0141*	0.446	*0.0018*	0.372	*0.0055*
dNBR	0.745	*0.0000*	0.860	*0.0000*	0.823	*0.0000*
RdNBR	0.773	*0.0000*	0.861	*0.0000*	0.836	*0.0000*
Extended Assessment						
d7/4 Ratio	0.528	*0.0004*	0.501	*0.0007*	0.532	*0.0004*
d7/5 Ratio	0.465	*0.0013*	0.456	*0.0015*	0.475	*0.0011*
dKTB	0.461	*0.0014*	0.668	*0.0000*	0.563	*0.0002*
dKTG	0.566	*0.0002*	0.590	*0.0001*	0.589	*0.0001*
dKTW	0.026	*0.5076*	0.130	*0.1302*	0.067	*0.2847*
dCHAR	0.340	*0.0087*	0.432	*0.0022*	0.389	*0.0043*
dPV	0.073	*0.2630*	0.116	*0.1533*	0.090	*0.2118*
dNPV	0.423	*0.0026*	0.505	*0.0007*	0.474	*0.0011*
dNBR	0.740	*0.0000*	0.789	*0.0000*	0.783	*0.0000*
RdNBR	0.776	*0.0000*	0.835	*0.0000*	0.823	*0.0000*

produced the strongest correlation to the Extended Assessment (EA) SUB ($R^2 = 0.776$, $p < 0.0001$). The same pattern emerged for the CBI metric, with $R^2 = 0.863$ ($p < 0.0001$) between dKTG and CBI for the L-L and IA pairs, and $R^2 = 0.823$, ($p < 0.0001$) between RdNBR and the EA pair. In comparison, dKTG produced the strongest correlation to SURF only for the IA pair ($R^2 = 0.872$, $p < 0.0001$), with dNBR most strongly correlated to SURF for the L-L pair ($R^2 = 0.880$, $p < 0.0001$) and RdNBR most strongly correlated for the EA pair ($R^2 = 0.835$, $p < 0.0001$).

The Spearman rank correlation found weaker links between spectral indices and burn severity metrics, but found the same general correlations to be significant at the $p < 0.001$ level. The strongest rank correlation was produced between RdNBR and the SURF metric of severity ($R^2 = 0.639$, $p < 0.0001$) for the L-L image pair. All relationships between the 3 severity metrics and both the dNBR and RdNBR metrics were significant at the $p < 0.001$ level, excepting the EA pair dNBR correlation to the CBI ($R^2 = 0.423$, $p = 0.0013$). The dKTG produced the strongest correlations to SUB for both the L-L and IA image pairs, but the EA pair dKTG was not significantly correlated to any of the severity metrics.

ASSESSMENT OF DOWNSAMPLED MODIS DATA

Spectral indices produced from both the Initial and Extended Assessment image pairs were significantly correlated to CBI data with similar correlation coefficients (Tables 3 and 4), with d7/4, dKTG, dNBR, and RdNBR producing the strongest correlations depending on image pair and metric. A confusion matrix cross-tabulating dNBR classes between the Initial Assessment and the Extended Assessment reveals class changes consistent with the vegetation regeneration observed on the tundra (i.e., green-up) (Table 5). A decrease in severity class was observed across 41.5% of pixels, including decreases in severity from extreme to high (25.4%), extreme to moderate (1.1%), high to moderate (7.7%), high to low (0.2%), moderate to low (4.4%), moderate to unburned (0.4%), and low to unburned (2.3%). We calculated that 51.6% of

TABLE 4

Spearman rank correlations (R^2) between the 10 spectral metrics and the 3 metrics of burn severity: Surface (SURF), Substrate (SUB), and Composite Burn Index (CBI). Correlations with *p*-values less than 0.001 are considered highly significant.

	SUB		SURF		CBI	
	R^2	*p*	R^2	*p*	R^2	*p*
Landsat-only pair						
d7/4 Ratio	0.436	*0.0010*	0.641	*0.0000*	0.517	*0.0003*
d7/5 Ratio	0.315	*0.0060*	0.464	*0.0007*	0.348	*0.0039*
dKTB	0.145	*0.0536*	0.313	*0.0064*	0.185	*0.0327*
dKTG	0.469	*0.0006*	0.523	*0.0002*	0.489	*0.0004*
dKTW	0.038	*0.2118*	0.134	*0.0618*	0.051	*0.1753*
dCHAR	0.104	*0.0898*	0.189	*0.0315*	0.119	*0.0734*
dPV	0.000	*0.4764*	0.003	*0.4142*	0.394	*0.3990*
dNPV	0.177	*0.0366*	0.177	*0.0366*	0.155	*0.0527*
dNBR	0.459	*0.0007*	0.625	*0.0000*	0.532	*0.0002*
RdNBR	0.450	*0.0008*	0.639	*0.0000*	0.525	*0.0002*
Initial Assessment						
d7/4 Ratio	0.438	*0.0010*	0.641	*0.0000*	0.517	*0.0003*
d7/5 Ratio	0.247	*0.0152*	0.430	*0.0012*	0.284	*0.0093*
dKTB	0.145	*0.0537*	0.313	*0.0064*	0.185	*0.0327*
dKTG	0.469	*0.0006*	0.523	*0.0002*	0.489	*0.0004*
dKTW	0.038	*0.2118*	0.134	*0.0618*	0.051	*0.1753*
dCHAR	0.007	*0.3690*	0.180	*0.0352*	0.038	*0.2118*
dPV	0.080	*0.1196*	0.001	*0.4568*	0.031	*0.2347*
dNPV	0.000	*0.4843*	0.083	*0.1159*	0.004	*0.3952*
dNBR	0.454	*0.0008*	0.613	*0.0000*	0.520	*0.0002*
RdNBR	0.459	*0.0007*	0.639	*0.0000*	0.531	*0.0002*
Extended Assessment						
d7/4 Ratio	0.469	*0.0006*	0.412	*0.0015*	0.439	*0.0010*
d7/5 Ratio	0.306	*0.0070*	0.176	*0.0373*	0.303	*0.0073*
dKTB	0.163	*0.0432*	0.435	*0.0011*	0.263	*0.0125*
dKTG	0.174	*0.0380*	0.281	*0.0097*	0.207	*0.0250*
dKTW	0.015	*0.3049*	0.164	*0.0432*	0.059	*0.1565*
dCHAR	0.072	*0.1330*	0.138	*0.0586*	0.084	*0.1141*
dPV	0.000	*0.4647*	0.004	*0.4028*	0.002	*0.4219*
dNPV	0.121	*0.0722*	0.112	*0.0799*	0.105	*0.0868*
dNBR	0.447	*0.0009*	0.466	*0.0006*	0.423	*0.0013*
RdNBR	0.469	*0.0006*	0.412	*0.0015*	0.439	*0.0010*

TABLE 5

Confusion matrix indicating the proportional change by class in burn severity across the landscape between the Initial and Extended Assessments.

		Initial Assessment					
		UNB	LOW	MOD	HIGH	EXT	Total
Extended Assessment	UNB	0.009	0.023	0.004	0.000	0.000	0.036
	LOW	0.002	0.066	0.044	0.002	0.000	0.114
	MOD	0.000	0.004	0.049	0.077	0.011	0.141
	HIGH	0.000	0.000	0.009	0.119	0.254	0.382
	EXT	0.000	0.000	0.000	0.008	0.318	0.327
	Total	0.011	0.093	0.106	0.206	0.584	1

the area was unchanged from the Initial to the Extended Assessment, while 2.3% was classified as more severe in the Extended Assessment than in the Initial. In the Initial Assessment, nearly 80% of the area within the fire perimeter was classified as High to Extreme Severity, while only 20% was classified as Low or Moderate Severity. By the Extended Assessment in July, only 71% of the area was classified as High to Extreme Severity, while 25% was classified as Low to Moderate Severity, and less than 4% was classified as Unburned (up from $<1\%$ in the Initial Assessment).

Discussion

Several spectral indices tested here showed significant correlations to the plot data, with the strength of the correlation depending on the metric and the index. Correlations to spectral data were strongest with the Surface metric, and weakest with the Substrate metric, with CBI balancing the two. This supports previous findings in boreal Alaska ecosystems that spectral indices perform poorly representing consumption of substrate organic horizons (Kasischke et al., 2008; Hoy et al., 2008), and that CBI relationships to spectral indices are primarily surface relationships with vegetation consumption (Miller et al., 2009). This is well-demonstrated in the correlations to dKTG across the three image pairs; dKTG is significantly correlated to CBI metrics for the L-L and the IA image pairs, which utilize the June post-fire image, captured before the summer 2008 green-up began. The dKTG is poorly correlated to CBI for the EA, however, which is consistent with ground observations that many burned areas had begun to regenerate (i.e., re-green) by the July EA. Spectral metrics for d7/4 and dKTG were both significantly correlated to some components of the assessment, but only the dNBR and RdNBR were consistently significantly correlated across all image pairs and metrics.

While the number of CBI points was less than would normally be desired for like studies, the small n of field observations this study (19) illustrates well the challenges faced by researchers collecting field data in the most remote portions of Alaska. Researchers were only able to collect these data at a considerable expense, and the rapid green-up of the short arctic growing season severely limits the amount of time available to collect consistent field observations not reflecting a significant vegetation change over the time required to obtain them (e.g., a week's worth of rapid vegetation growth between first and last plots collected). Based on the small size of the CBI data set, and the clustering of the data into an unburned to low severity group and a high to extreme severity group (with no plots found in the moderate severity range of CBI), the authors acknowledge that a larger data set may reveal different links between tundra fire effects and spectral indices. However, we also suggest that the more robust Rank Correlation still shows significant relationships between CBI and spectral indices, and we additionally compare our results to another study of tundra fire severity to further assess the utility of the dNBR.

Our dNBR correlation with CBI ($R^2 = 0.82$ for Initial Assessment) complements previous work in Alaskan tundra that found strong correlations ($R^2 = 0.77$ to 0.78) between dNBR and CBI on 3 predominantly low-severity fires in the Bering tundra of western Alaska (Allen and Sorbel, 2008). CBI values occur along a scale of 0 to 3, and most of the Anaktuvuk River Fire burned at higher severity (all associated burned area CBI values exceeded 1.5) (Fig. 3). In an assessment of tundra burn severity presented by Allen and Sorbel (2008), the majority of their CBI points had a value below 1.5. Allen and Sorbel (2008) specifically noted that their high CBI-dNBR correlations might have resulted from their 3 tundra fires burning primarily at low severity, and that higher severity fires might yield a lower correlation to dNBR. However, when the CBI data from Allen and Sorbel (2008) are combined with the CBI plots from this study to represent the entire spectrum of tundra burn severity from low to high ($n = 112$), the combined CBI values are significantly correlated to dNBR ($R^2 = 0.69$, $p < 0.0001$) (Fig. 4). The strength of this correlation between CBI and dNBR across 2 distinct tundra regions is further evidence of the utility of dNBR for mapping surface burn severity on Alaskan tundra sites. It also further justifies the classification of the dNBR image for assessing the downsampled MODIS data.

CBI correlations to spectral indices were strongest for the L-L image pair, reaffirming that the use of Landsat data is the most preferable for mapping and monitoring fire impacts. However, when Landsat data are not available for all desired periods, the relationships between CBI and the EA spectral indices, as well as the patterns of dNBR classification revealed in the confusion matrix (Table 5) indicate that MODIS downsampling can provide supplemental information. The decrease in severity across over 40% of pixels (as compared to an illogical increase in severity for $<3\%$ of pixels) is consistent with both the ecology of the tussock tundra and the observations of rapid vegetation regeneration in the first growing season following the fire (Jandt, 2008). Cottongrass sedge has been observed to rapidly resprout after fire in Alaska (Racine

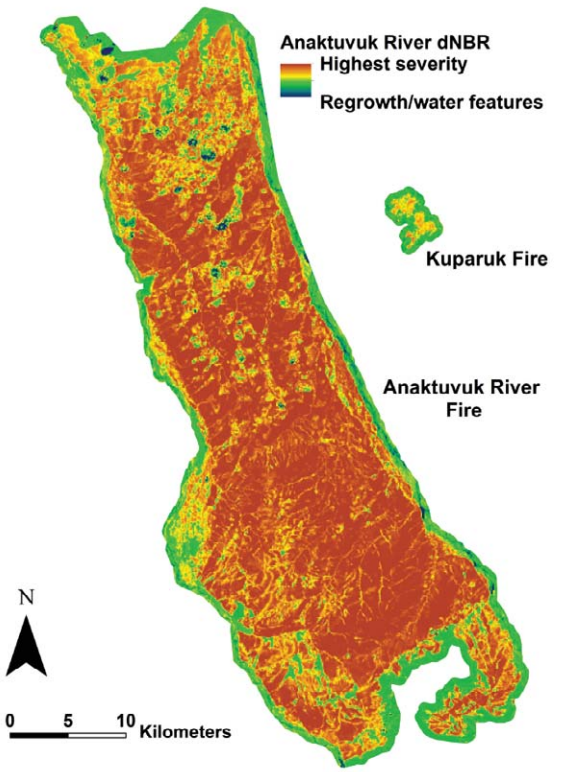

FIGURE 3. Final Initial Assessment dNBR (differenced Normalized Burn Ratio) map for the Anaktuvuk River Fire, with Kuparuk Fire (also burned in 2007) for comparison.

et al., 2004), and observations of cottongrass sedge tussocks in the burned area during the Initial and Extended Assessments indicated that while all of the leafy foliage burned, the tightly bundled roots at the center of the tussock retained too much moisture to be entirely consumed by the fire (Jandt, 2008). As described in the scene model section above, these root bundles rapidly resprouted after the June 2008 thaw and were contributing a significant green element to the scene by the July EA, lowering the severity of two-fifths of the burned area. That this change was captured by the downsampled

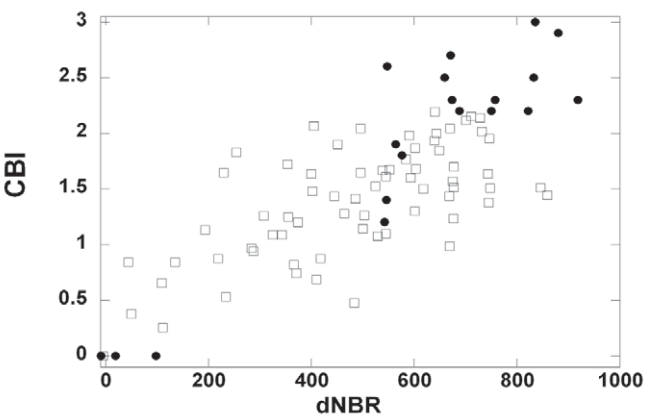

FIGURE 4. All Composite Burn Index (CBI) plots from Anaktuvuk River Fire (solid circles) and three fires from Allen and Sorbel (2008) (open squares) regressed to dNBR value for associated pixel, with regression line ($y = 0.0023x + 0.3144$).

July MODIS data, when no cloud-free Landsat images were available, signifies the utility of downsampled MODIS for temporal monitoring of fire effects.

These results come on the heels of findings from Boelman et al. (2011), who analyzed the same wildfire using the same ground observation points with the goal of assessing single-date imagery for mapping burn severity in a region where anniversary-date images are often difficult to acquire. They suggest that a potential solution to the inherent challenges of producing dNBR from matched-date imagery is to use the EVI2 spectral index with a single, post-fire image from any sensor with bands in the visible spectrum, and they also find that coarse-resolution MODIS data are too coarse for accurate burn severity mapping. While the single-date approach has been suggested previously in Alaska (e.g., Epting et al., 2005; Hudak et al., 2007), it fails to account for unburned inclusions such as rocks and small lakes that tend to be misclassified as high severity burned area in single-date scenes and must be mapped out in a labor-intensive process (Key, 2006). Since ground observation plots are never established in lakes or on rocks, validation analyses fail to account for this misclassification. We show here that by downsampling MODIS to the finer resolution of Landsat (30 m), both the coarse-resolution problem and the infrequency of Landsat are solved, while minimizing classification errors associated with single-date imagery.

Conclusions

The Anaktuvuk River Fire was a record fire that burned primarily at high severity (Fig. 3) in contrast with previous tundra fires in Alaska, provoking interest in the potential impacts of climate change on high-latitude fire regimes. The Anaktuvuk River Fire also drew much attention from researchers addressing issues of increased potential for carbon contributions from wildfires (Mack et al., 2011), impacts on the Central Arctic Caribou Herd and other wildlife, and impacts on the gas and oil extraction industry. Given the need to address these issues in light of projections that include further warming in the region, it is critical to explore methods for measuring and monitoring wildfire characteristics in this region, and to focus on developing methods that are accurate, efficient, and accessible to fire managers.

The results of this study indicate that several Landsat metrics easily produced by federal fire managers familiar with Geographic Information Systems are highly correlated to ground measurements of CBI. Bi-temporal spectral indices, including dKTG, dNBR, and RdNBR, produced significant correlations with CBI metrics, with the strongest correlations to the Surface metric. Downsampling of MODIS data shows promise for mapping wildfire burn severity where Landsat data are limited or not available, with the Extended Assessment in this study produced entirely from downsampled MODIS (i.e., both pre- and post-fire) and showing changes in severity from the Initial Assessment that are consistent with observations and tundra ecology. Field data are always the most desirable approach to monitoring disturbance impacts, and are absolutely necessary to interpreting the patterns identified in remotely sensed imagery. Overall, we show that remotely sensed data can be used in conjunction with field data to monitor impacts across the entire extent of the disturbance event, and that existing methods can be applied to characterize wildfire impacts from 2 different remotely

sensed data platforms in tundra ecotypes. This fills a critical monitoring need in the rapidly changing Arctic.

Acknowledgments

This project was funded by the USGS Land Remote Sensing program; field data were provided by Alaska Fire Service. The authors are grateful to Nancy French, Kirsten Barrett, and two anonymous reviews for significantly improving the manuscript, and to Randi Jandt for photos and contributions. Any use of trade, product, or firm names is for descriptive purposes only and does not imply endorsement by the U.S. Government.

References Cited

AFS [Alaska Fire Service], 2009: Alaska Large Fire History database. http://fire.ak.blm.gov/, accessed 9 May 2009.

Allan, G. E., 1993: *The Fire History of Central Australia*. Alice Springs, Australia: CSIRO/CCNT Technical Report, Bushfire Research Project, v. 4.

Allen, J. L., and Sorbel, B., 2008: Assessing the differenced normalized burn ratio's ability to map burn severity in the boreal forest and tundra ecosystems of Alaska's national parks. *International Journal of Wildland Fire*, 17: 463–475.

Apps, M. J., Kurz, W. A., Luxmore, R. J., Nilsson, L. O., Sedjo, R. A., Schmidt, R., Simpson, L. G., and Vinson, T. S., 1993: Boreal forests and tundra. *Water, Air, and Soil Pollution*, 70: 39–53.

Boelman, N. T., Rocha, A. V., and Shaver, G. R., 2011: Understanding burn severity in arctic tundra: exploring vegetation indices, suboptimal assessment timing and the impact of increasing pixel size. *International Journal of Remote Sensing*, 32: 7033–7056, http://dx.doi.org/10.1080/01431161.2011.611187.

Bogdanov, A. V., Sandven, S., Johannessen, O. M., Alexandrov, V. Y., and Bobylev, L. P., 2005: Multisensor approach to automated classification of sea ice image data. *IEEE Transactions on Geoscience and Remote Sensing*, 43(7): 1648–1663.

Chander, G., and Markham, B., 2003: Revised Landsat-5 TM radiometric calibration procedures and post-calibration dynamic ranges. *IEEE Transactions on Geoscience and Remote Sensing*, 41(11): 2674–2677.

Chapin, F. S., III, Sturm, M., Serreze, M. C., McFadden, J. P., Key, J. R., Lloyd, A. H., McGuire, A. D., Rupp, T. S., Lynch, A. H., Schimmel, J. P., Beringer, J., Chapman, W. L., Epstein, H. E., Euskirchen, E. S., Hinzman, L. D., Jia, G., Ping, C.-L., Tape, K. D., Thompson, C. D. C., Walker, D. A., and Welker, J. M., 2005: Role of land-surface changes in arctic summer warming. *Science*, 310(5748): 657–660, http://dx.doi.org/10.1126/science.1117368.

Chapin, F. S., III, Oswod, M. W., Van Cleve, K., Viereck, L. A., and Verbyla, D. L. (eds.), 2006: *Alaska's Changing Boreal Forest*. New York: Oxford University Press, 354 pp.

Chavez, P., Jr., 1996: Image-based atmospheric corrections—Revised and improved. *Photogrammetric Engineering and Remote Sensing*, 62: 1025–1036.

Clark Labs, 2010: IDRISI Taiga software system. Worcester, Massachusetts: Clark Labs.

Cosimo, J. C., 2006: Warming trends in the Arctic from clear sky satellite observations. *Journal of Climate*, 16: 3498–3510.

Curry, J. C., 1996: *A time series analysis of the spectral response of fire and vegetation regrowth in Landsat imagery of Australia's Great Victoria Desert: an initial analysis*. M.S. thesis, University of Texas at Austin.

De Santis, A., and Chuvieco, E., 2009: GeoCBI: a modified version of the Composite Burn Index for the initial assessment of the short-term burn severity from remotely sensed data. *Remote Sensing of Environment*, 113(3): 554–562.

Durner, G. M., Douglas, D. C., Nielson, R. M., Amstrup, S. C., McDonald, T. L., Stirling, I., Mauritzen, M., Born, E. W., Wiig, Ø., DeWeaver, E., Serreze, M., Belikov, S. E., Holland, M. M., Maslanik, J., Aars, J., Bailey, D. A., and Derocher, A. E., 2009: Predicting 21st-century polar bear habitat distribution from global climate models. *Ecological Monographs*, 79(1): 25–58, http://dx.doi.org/10.1890/07-2089.1.

Eidenshink, J., Schwind, B., Brewer, K., Zhu, Z., Quayle, B., and Howard, S., 2007: A project for monitoring trends in burn severity. *Fire Ecology*, 3(1): 3–21.

Epting, J., Verbyla, D., and Sorbel, B. 2005: Evaluation of remotely sensed indices for assessing burn severity in interior Alaska using Landsat TM and ETM+. *Remote Sensing of Environment*, 96: 328–339.

French, N. H. F, Kasischke, E. S., Hall, R. J., Murphy, K. A., Verbyla, D. L., Hoy, E. E., and Allen, J. L., 2008: Using Landsat data to assess fire and burn severity in the North American boreal forest region: an overview and summary of results. *International Journal of Wildland Fire*, 17: 443–462.

Gao, F., Masek, J., Schwaller, M., and Hall, F., 2006: On the blending of the Landsat and MODIS surface reflectance: predicting daily Landsat surface reflectance. *IEEE Transactions on Geoscience and Remote Sensing*, 44(8): 2207–2218.

Higuera P. E., Brubaker L. B., Anderson P. M., Brown T. A., Kennedy A. T., and Hu, F. S., 2008: Frequent fires in ancient shrub tundra: implications of paleorecords for arctic environmental change. *PLoS ONE*, 3(3): e0001744, http://dx.doi.org/10.1371/journal.pone.0001744.

Hinzman, L. D., Bettez, N. D., Bolton, W. R., Chapin, F. S., Dyurgerov, M. B., Fastie, C. L., Griffith, B., Hollister, R. D., Hope, A., Huntington, H. P., Jensen, A. M., Jia, G. J., Jorgenson, T., Kane, D. L., Klein, D. R., Kofinas, G., Lynch, A. H., Lloyd, A. H., McGuire, A. D., Nelson, F. E., Oechel, W. C., Osterkamp, T. E., Racine, C. H., Romanovsky, V. E., Stone, R. S., Stow, D. A., Sturm, M., Tweedie, D. A., Webber, P. J., Welker, J. M., Winker, K. S., and Yoshikawa, K., 2005: Evidence and implications of recent climate change in northern Alaska and other arctic regions. *Climatic Change*, 72: 251–298, http://dx.doi.org/10.1007/s10584-005-5352-2.

Homer, C., Dewitz, J., Fry, J., Coan, M., Hossain, N., Larson, C., Herold, N., McKerrow, A., VanDriel, J. N., and Wickham, J., 2007: Completion of the 2001 National Land Cover Database for the conterminous United States. *Photogrammetric Engineering and Remote Sensing*, 73(4): 337–341.

Hoy, E. E., French, N. H. F., Turetsky, M. R., Trigg, S. N., and Kasischke, E. S., 2008: Evaluating the potential of Landsat TM/ETM+ imagery for assessing fire severity in Alaskan black spruce forests. *International Journal of Wildland Fire*, 17: 500–514.

Hu, F. S., Higuera, P. E., Walsh, J. E., Chapman, W. L., Duffy, P. A., Brubaker, L. B., and Chipman, M. L., 2010: Tundra burning in Alaska: linkages to climatic change and sea-ice retreat. *Journal of Geophysical Research–Biogeosciences*, 115: G04002, http://dx.doi.org/10.1028/2009JG001270.

Huang, C., Wylie, B., Yang, L., Homer, C., and Zylstra, G., 2001: *Derivation of a tasseled cap transformation based on Landsat 7 at-satellite reflectance*. Sioux Falls, South Dakota: Raytheon ITSS, USGS EROS Data Center.

Hudak, A. T., Lewis, S., Robichaud, P., Morgan, P., Bobbitt, M., Lentile, L., Holden, Z., Clark, J., and McKinley, R., 2006: Sensitivity of Landsat image-derived burn severity indices to immediate post-fire effects. *In* Association for Fire Ecology, *Proceedings of the 3rd Fire Ecology and Management Congress, San Diego, California, November 2006.*

Hudak, A. T., Morgan, P., Bobbitt, M. J., Smith, A. M. S., Lewis, S. A., Lentile, L. B., Robichaud, P. R., Clark, J. T., and McKinley, R. A., 2007: The relationship of multispectral satellite imagery to immediate fire effects. *Fire Ecology*, 3(1): 64–90.

Intrieri, J., Shupe, M. D., Uttal, T., and McCarty, B. J., 2002: An annual cycle of arctic cloud characteristics observed by radar and lidar at SHEBA. *Journal of Geophysical Research*, 107: 1–17.

IPCC, 2007: *Climate Change 2007: the Physical Science Basis. Contri-*

bution of Working Group I to the Fourth Assessment Report of the Intergovernmental Panel on Climate Change. [Solomon, S., Qin, D., Manning, M., Chen, Z., Marquis, M., Averyt, K. B., Tignor, M., Miller, H. L. (eds.)]. Cambridge: Cambridge University Press.

Jandt, R. R., 2008: *Field trip report on 2007 North Slope fire study*. Bureau of Land Management unpublished report, July 15, 2008, 5 pp.

Jandt, R. R., and Myers, C. R., 2000: *Recovery of lichen in tussock tundra following fire in northwestern Alaska*. Anchorage, Alaska: BLM Alaska State Office, Bureau of Land Management–Alaska Open File Report 82, 30 pp.

Jones, B. J., Kolden, C. A., Jandt, R. R., Abatzoglou, J. T., Urban, F., and Arp, C. D., 2009: Fire behavior, weather, and burn severity of the 2007 Anaktuvuk River tundra fire, North Slope, Alaska. *Arctic, Antarctic, and Alpine Research*, 41(3): 309–316.

Kasischke, E. S., 2000: Boreal ecosystems in the global carbon cycle. *In* Kasischke, E. S., and Stocks, B. J. (eds.), *Fire, Climate Change, and Carbon Cycling in the Boreal Forest*. New York: Springer-Verlag, 19–30.

Kasischke, E. S., and Stocks, B. J. (eds.), 2000: *Fire, Climate Change, and Carbon Cycling in the Boreal Forest*. New York: Springer-Verlag.

Kasischke, E. S., Turetsky, M. R., Ottmar, R. D., French, N. H. F., Hoy, E. E., and Kane, E. S., 2008: Evaluation of the composite burn index for assessing fire severity in Alaskan black spruce forests. *International Journal of Wildland Fire*, 17*:* 515–526.

Kaufman, Y. J., Ichoki, C., Giglio, L., Korontzi, S., Chu, D. A., Hao, W. M., Li, R.-R., and Justice, C. O., 2003: Fire and smoke observed from the Earth Observing System MODIS instrument—Products, validation, and operational use. *International Journal of Remote Sensing*, 24(8): 1765–1781.

Keeley, J. E., 2009: Fire intensity, fire severity and burn severity: a brief review and suggested usage. *International Journal of Wildland Fire*, 18: 116–126.

Key, C. H., 2006: Ecological and sampling constraints on defining landscape fire severity. *Fire Ecology*, 2(2): 1–26.

Key, C. H., and Benson, N. C., 2006: Landscape assessment: ground measure of severity, the Composite Burn Index; and remote sensing of severity, the Normalized Burn Ratio. *In* Lutes, D. C., Keane, R. E., Caratti, J. F., Key, C. H., Benson, N. C., Sutherland, S., and Gangi, L. J. (eds.), *FIREMON: Fire Effects Monitoring and Inventory System*. Ogden, Utah: USDA Forest Service, Rocky Mountain Research Station, General Technical Report RMRS-GTR-164-CD: LA1–LA51, http://frames.nbii.gov/projects/firemon/FIREMON LandscapeAssessment.pdf.

Liljedahl, A., Hinzman, L., Busey, R., and Yoshikawa, K., 2007: Physical short-term changes after a tussock tundra fire, Seward Peninsula, Alaska. *Journal of Geophysical Research–Earth Surface*, 112: http://dx.doi.org/10.1029/2006JF000554.

Lloyd, A. H., and Fastie, C. L., 2003: Recent changes in tree line forest distribution and structure in interior Alaska. *Ecoscience*, 10: 176–185.

Mack, M. C., Bret-Harte, M. S., Hollingsworth, T. N., Jandt, R. R., Schuur, E. A. G., Shaver, G. R., and Verbyla, D. L., 2011: Carbon loss from an unprecedented arctic tundra wildfire. *Nature*, 475: 489–492, http://dx.doi.org/10.1038/nature10283.

Markon, C. J., 2001: *Seven-year phenological record of Alaskan ecoregions derived from Advanced Very High Resolution Radiometer Normalized Differenced Vegetation Index*. Anchorage, Alaska: USGS Open-File Report 01-11, 58 pp.

Mather, P. M., 1989: *Computer Processing of Remotely-Sensed Images: an Introduction*. New York: Wiley.

Miller, J. D., and Thode, A. E., 2007: Quantifying burn severity in a heterogeneous landscape with a relative version of the delta Normalized Burn Ratio (dNBR). *Remote Sensing of Environment*, 109: 66–80.

Miller, J. D., Knapp, E. E., Key, C. H., Skinner, C. N., Isbell, C. J., Creasy, R. M., and Sherlock, J. W., 2009: Calibration and validation of the relative differenced Normalized Burn Ratio (RdNBR) to three measures of fire severity in the Sierra Nevada and Klamath Mountains, California, USA. *Remote Sensing of Environment*, 113(3): 645–656.

Murphy, K. A., and Witten, E., 2008: Tussock tundra 2. *In* Hann, W., Shlisky, A., Havlina, D., Schon, K., Barrett, S., DeMeo, T., Pohl, K., Menakis, J., Hamilton, D., Jones, J., Levesque, M., and Frame, C. (eds.), 2004: *Interagency Fire Regime Condition Class Guidebook*. Last update January 2008: Version 1.3.0 [Homepage of the Interagency and The Nature Conservancy fire regime condition class website, USDA Forest Service, U.S. Department of the Interior, The Nature Conservancy, and Systems for Environmental Management], http://www.frcc.gov.

Murphy, K. A., Reynolds, J. H., and Koltun, J. M., 2008: Evaluating the ability of the difference Normalized Burn Ratio (dNBR) to predict ecologically significant burn severity in Alaskan boreal forests. *International Journal of Wildland Fire*, 17: 490–499.

O'Neill, S. J., Osborne, T. J., Hulme, M., Lorenzoni, I., and Watkinson, A. R., 2008: Using expert knowledge to assess uncertainties in future polar bear populations under climate change. *Journal of Applied Ecology*, 45(6): 1649–1659, http://dx.doi.org/10.1111/j.1365-2664.2008.01552.x.

Quirino, V. F., Wynne, R. H., Liu, X., and Blinn, C. E., 2008: Downscaling the MODIS NDVI product for pine ecosystem productivity estimates. In *Proceedings of the 2008 IEEE International Geoscience and Remote Sensing Symposium, July 6–11, 2008, Boston, Mass., USA*. http://www.igarss08.org/Abstracts/pdfs/3894.pdf, last accessed 26 November 2012.

Racine, C., Jandt, R., Meyers, C., and Dennis, J., 2004: Tundra fire and vegetation change along a hillslope on the Seward Peninsula, Alaska, U.S.A. *Arctic, Antarctic, and Alpine Research*, 36(1): 1–10.

Racine, C. H., Johnson, L. A., and Viereck, L. A., 1987: Patterns of vegetation recovery after tundra fires in northwestern Alaska, U.S.A. *Arctic and Alpine Research*, 19: 461–469.

Roberts, D. A., Gardner, M., Church, R., Ustin, S., Scheer, G., and Green, R. O., 1998: Mapping chaparral in the Santa Monica Mountains using multiple endmember spectral mixture models. *Remote Sensing of Environment*, 65: 267–279.

Rogan, J., and Franklin, J., 2001: Mapping wildfire severity in southern California using spectral mixture analysis. In *Proceedings: Geoscience and Remote Sensing Symposium, 2001. IGARSS '01. IEEE 2001 International*, vol. 4: 1681–1683.

Rogan, J., and Yool, S. R., 2001: Mapping fire-induced vegetation depletion in the Peloncillo Mountains, Arizona and New Mexico. *International Journal of Remote Sensing*, 22(16): 3101–3121.

Rogan, J., Franklin, J., and Roberts, D. A., 2002: A comparison of methods for monitoring multitemporal vegetation change using Thematic Mapper imagery. *Remote Sensing of Environment*, 80: 143–156.

Russell-Smith, J., and Yates, C. P., 2007: Australian savanna fire regimes: context, scales, patchiness. *Fire Ecology*, 3(1): 48–63.

Serreze, M. C., Walsh, J. E., Chapin, F. S., Osterkamp, T., Dyurgerov, M., Romanovsky, V., Oechel, W. C., Morison, J., Zhang, T., and Barry, R. G., 2000: Observational evidence of recent change in the northern high-latitude environment. *Climatic Change*, 46 (1–2): 159–207, http://dx.doi.org/10.1023/A:1005504031923.

Shulski, M., and Wendler, G., 2007: *The Climate of Alaska*. Fairbanks, Alaska: University of Alaska Press, 216 pp.

Stow, D. A., Hope, A., McGuire, D., Verbyla, D., Gamon, J., Huemmrich, F., Houston, S., Racine, C., Sturm, M., Tape, K., Hinzman, L., Yoshikawa, K., Tweedie, C., Noyle, B., Silapaswan, C., Douglas, D., Griffith, B., Jia, G., Epstein, H., Walker, D., Daeschner, S., Peterson, A., Zhou, L., and Myneni, R., 2004: Remote sensing of vegetation and land-cover change in arctic tundra ecosystems. *Remote Sensing of Environment*, 89: 281–308.

Strahler, A. H., Woodcock, C. E., and Smith, J. A., 1986: On the nature of models in remote sensing. *Remote Sensing of Environment*, 20: 121–139.

Sturm, M., Douglas, T., Racine, C., and Liston, G. E., 2005: Changing snow and shrub conditions affect albedo with global implications.

Journal of Geophysical Research, 110: G01004, http://dx.doi.org/10.1029/2005JG000013.

USGS [U.S. Geological Survey], 2011: Processing description, http://landsat.usgs.gov/Landsat Processing Details.php.

Verbyla, D. L., and Boles, S. H., 2000: Bias in land cover change estimates due to misregistration. *International Journal of Remote Sensing*, 21(18): 3553–3560.

Verbyla, D. L., Kasischke, E. S., and Hoy, E. E., 2008: Seasonal and topographic effects on estimating fire severity from Landsat TM/ETM + data. *International Journal of Wildland Fire*, 17: 527–534.

Vermote, E. F., and Kotchenova, S., 2008: Atmospheric correction for the monitoring of land surfaces. *Journal of Geophysical Research*, 113: D23S90, http://dx.doi.org/10.1029/2007JD009662.

Viereck, L. A., Dyrness, C. T., Batten, A. R., and Wenzlick, K. J., 1992: *The Alaska Vegetation Classification*. Portland, Oregon: Pacific Northwest Research Station, USDA Forest Service General Technical Report PNW-GTR-286, 278 pp.

Walz, Y., Maier, S. W., Dech, S. W., Conrad, C., and Colditz, R. R., 2007: Classification of burn severity using Moderate Resolution Imaging Spectroradiometer (MODIS): a case study in the jarrah-marri forest of southwest Western Australia. *Journal of Geophysical Research*, 112: G02002, http://dx.doi.org/10.1029/2005JG000118.

Wein, R. W., 1976: Frequency and characteristics of arctic tundra fires. *Arctic*, 29: 213–222.

Wein, R. W., and MacLean, D. A. (eds.), 1983: *The Role of Fire in Northern Circumpolar Ecosystems*. New York: John Wiley and Sons, 322 pp.

White, J. D., Ryan, K. C., Key, C. C., and Running, S. W., 1996: Remote sensing of forest fire severity and vegetation recovery. *International Journal of Wildland Fire*, 6: 125–136.

Wilks, D. S., 1995: Statistical Methods in the Atmospheric Sciences. San Diego: Academic Press, 467 pp.

WRCC [Western Regional Climate Center], 2009: Alaska station data and historical summaries. http://www.wrcc.dri.edu, accessed 23 March 2009.

Zhu, Z., Key, C. H., Ohlen, D., and Benson, N. C., 2006: *Evaluating Sensitivities of Burn Severity Mapping Algorithms for Different Ecosystems and Fire Histories*. Boise, Idaho: Final Report to the Joint Fire Science Program.

MS accepted September 2012